

# A New Controller for PMSM Servo Drive Based on the Sliding Mode Approach with Parameter Adaptation

Orges Gjini\* Member

Takayuki Kaneko\* Member

Hiroshi Ohsawa\* Member

A novel controller based on the Sliding Mode (SM) approach is designed for controlling a permanent magnet synchronous motor (PMSM) in a servo drive. After analyzing the classical SM controller, changes are made in the controller design such that its performance is substantially improved. To improve the controller performance in steady state (zero error positioning) an integral block is added to the controller resulting in a new controller configuration, which we call Sliding Mode Integral (SMI) controller. The new controller is tuned based on the results from parameter identification of the motor and the working machine. To cope with model parameter variations, especially unpredictable friction changes, gain scheduling and fuzzy based adaptive techniques are used in the control algorithm. Experiments and simulations are carried out and their results show a high performance control. The new controller offers very good tracking; it is highly robust, reaches the final position very fast and has a large stall torque. Furthermore the application of the SM ensures reduction of the system order by one. For comparison, the new controller's performance is compared with that of a PI controller. From the experimental results it is obvious the superiority of the new proposed controller.

**Keywords:** Servo, Sliding Mode (SM), adaptive control, permanent magnet synchronous motor (PMSM).

## 1. Introduction

Sliding Mode Control (SMC) theory was introduced for the first time in the context of the variable structure systems (VSS). It has become so popular that now it represents this class of control systems. Even though, in its early stages of development, the SMC theory was overlooked because of the developments in the famous linear control theory, during the last 20 years it has shown to be a very effective control method.

It is an interesting fact that despite numerous theoretical studies and results based on computer simulations, successful application results are reported only in few cases. The main reasons are thought to be difficulties in implementation (calculation of derivatives etc.) and chattering in the control output. Further, in case of servo applications, relatively large steady state positioning errors become an obstacle.

In some studies, in order to reduce chattering in the control output, a deliberate increase by one, in the system order is applied by introduction of another control loop<sup>(3)</sup>. On the other hand, this deteriorates the tracking performance and robustness of the controller.

In case of the servo applications, a proper choice of the model order, precise reference input and care during implementation can overcome the problem of derivative calculations. As for the chattering problem and the

steady state positioning error, these are caused by the un-modeled dynamics, linearization and uncertainty in the model parameters.

This study shows that when SM is implemented with some adjustments and combined with adaptation techniques, it can result in a high performance servo system. While in the literature excessive studies describe and compare different control methodologies based on a single approach<sup>(2)</sup> like Fuzzy (FC), Neural Network (NN) or Sliding Mode (SM); it is our believe that a combination of different control methods in a single controller gives the best result. It is important to understand that, while the simplicity, fast response and robustness of the SM algorithms makes this theory particularly attractive for servo control applications; the newly developed NN, FC theories can support it in dealing with parameter and model uncertainties. Further, integral action remains the preferred choice for a zero steady state error.

In this paper, firstly we show modeling and experimental results of parameter identification, in case of fly-wheel and ball-screw table mechanism. Later on, we explain the design of the proposed SMI controller for the PMSM servo application with integral action and parameter adaptation techniques. Finally implementation and discussion of the experimental results are presented.

## 2. Plant model and identification

Considering the permanent magnet synchronous motor (PMSM), we can write the electromagnetic equations of the motor (in a, b, c coordinates) as following:

\* Fuji Electric Co. Research and Development Ltd.  
1, Fuji-machi, Hino-city, Tokyo 191-8502, Japan.

$$\begin{aligned} U &= R \cdot I + \frac{d\Psi}{dt} \\ \Psi &= L \cdot I + \Psi_M \end{aligned} \quad \dots\dots\dots (1)$$

$U, I, \Psi$ : voltage, current and flux vectors respectively  
 $R, L$ : resistance and inductance matrices respectively  
 $\Psi_M$ : permanent magnet flux vector

Neglecting the reluctance effect, in  $(d, q)$  coordinates the electromagnetic equations are written as following:

$$\begin{aligned} \frac{di_d}{dt} &= -\frac{R}{L}i_d + \omega_e i_q + \frac{1}{L}u_d \\ \frac{di_q}{dt} &= -\frac{R}{L}i_q - \omega_e i_d - \frac{1}{L}\lambda_0\omega_e + \frac{1}{L}u_q \end{aligned} \quad \dots\dots\dots (2)$$

and the torque equation:

$$\begin{aligned} \frac{d\omega_r}{dt} &= \frac{1}{J}(\tau_e - \tau_l - B\omega_r) \\ \frac{d\theta_r}{dt} &= \omega_r \\ \omega_e &= p \cdot \omega_r \end{aligned} \quad \dots\dots\dots (3)$$

$\tau_e = \frac{3}{2}p\lambda_0 i_q$ : Electrical torque of the motor

In the above equations:

$R$ : stator resistance [ohm]

$L$ : stator inductance ( $L_d=L_q=L$ ) [H]

$J$ : moment of inertia [ $\text{kg m}^2$ ]

$B$ : damping constant [N m/rad/s]

$\tau_l$ : load torque [N m]

$p$ : number of pole pairs

$\omega_r, \omega_e$ : rotor and electrical angular speeds [rad/s]. ( $\omega_e = p\omega_r$ )

$\lambda_0$ : the flux linkage of the permanent magnet [Vs / rad]

In Eq. (2), the term  $\lambda_0\omega_e = e_q$  represent the q-component of the electro-magnetic force (EMF) generated by the permanent magnet. The d-component of the EMF ( $e_d$ ) is equal to zero. If  $i_d$  component is controlled to be zero, we get a similar behavior with a dc motor Fig. 1.

A block diagram of the PMSM with ACR (Automatic Current Regulator) is shown in Fig. 1. Compensating for the q-component of the motor EMF ( $e_q$ ) as shown in the diagram in Fig. 1, considering the electrical time constant of the motor negligible compared to its mechanical time constant and the ACR loop very fast (4-5 times faster than the outer speed control loop), we can simplify the model as shown in Fig. 2.

Further by considering a rigid mechanism coupled to

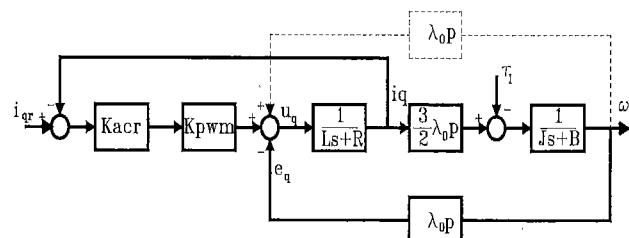


Fig. 1. Block diagram of the PMSM with ACR.

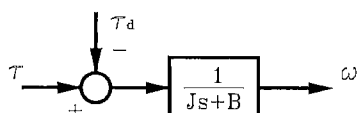


Fig. 2. Simplified block diagram of the plant.

the motor (a ball-screw table or a flywheel mechanism), we can approximate the plant (PMSM, mechanism and ACR) by a first order transfer function too. This transfer function is estimated by an identification procedure that follows. The main advantage in choosing this model is that a simple identification algorithm can be used to determine its parameters, which can be implemented in a low cost servo amplifier. The un-modeled dynamics and parameter uncertainty from the identification are overcome by the robustness of the controller and the adaptive algorithm implemented in it.

To carry out the identification process a step input is applied to the model shown in Fig. 2. The speed response of the plant is recorded. Based on the best fitting of the response with a first order step response, parameters  $J$  and  $B$  are estimated. These parameters correspond to the total plant model and are different from those in Eq.5, which belong to the motor model only. Estimated values of  $J$  and  $B$  of the first order model are shown in Tab.1. Aside them are shown the calculated values of load ( $J_M + J_L$ ).

In Fig. 3 to Fig. 5 are shown the plant responses and the estimated model responses together with the input torque step. The vertical axis in Fig. 3 to Fig. 5 is scaled in [%], where 3000 rpm and 0.637 Nm represent 100% levels for the speed and torque respectively.

Both parameters  $J$  and  $B$  are estimated by minimizing the following criterion:

$$S = \frac{1}{N} \sum_{k=0}^{N-1} [(y(kT) - \hat{y}(kT))]^2 \quad \dots\dots\dots (4)$$

Because parameter  $B$  can be determined directly from the steady state values of input and output from identification, the only parameter to be found from minimization is  $J$ . This is done simply by searching successively to find the best value of  $J$ , which minimizes the criterion (4).

Table 1. Estimated and calculated model parameters.

Load type	Calculated	Estimated	
	$J$ [ $\text{kg m}^2$ ]	$J$ [ $\text{kg m}^2$ ]	$B$ [Nm/rad/sec]
No-load	$2.16 \times 10^{-5}$	$2.77 \times 10^{-5}$	$5.689 \times 10^{-4}$
Flywheel-1	$9.01 \times 10^{-5}$	$12.1 \times 10^{-5}$	$5.660 \times 10^{-4}$
Flywheel-2	$30.0 \times 10^{-5}$	$33.9 \times 10^{-5}$	$5.720 \times 10^{-4}$
Ball-screw	$8.70 \times 10^{-5}$	$8.06 \times 10^{-5}$	$33.75 \times 10^{-4}$

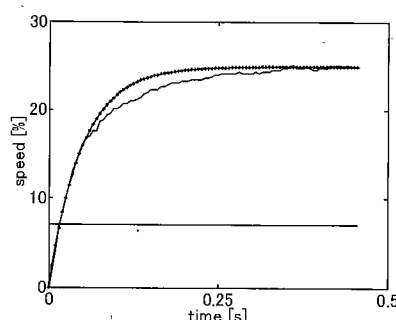


Fig. 3. Plant and model response at no-load.

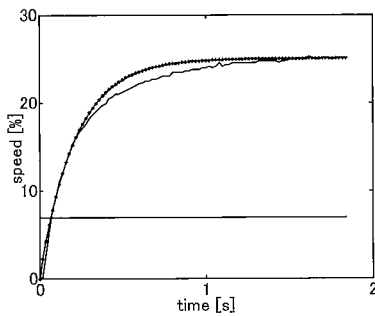


Fig. 4. Plant and model response flywheel-1.

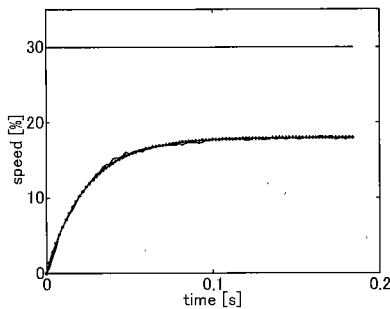


Fig. 5. Plant and model response ball-screw table.

### 3. The Sliding Mode Integral (SMI) Controller

In this section we will show first the design of the SM controller and later, based on the analysis and interpretation of the controller block diagram we introduce the proposed SMI controller.

The simplified motor model equations, deduced in the previous section, are written as:

$$\begin{cases} \dot{x}_1 = x_2 \\ \dot{x}_2 = -\frac{B}{J} \cdot x_2 + \frac{1}{J} \tau - \frac{1}{J} \tau_d \end{cases} \quad (5)$$

$$\begin{aligned} x_1 &= \theta \\ x_2 &= \omega \\ \ddot{\theta} &= -\frac{B}{J} \cdot \dot{\theta} + \frac{1}{J} \tau - \frac{1}{J} \tau_d \end{aligned} \quad (6)$$

$J, B$ : estimated model parameters (from section. 3)  
 $\theta, \theta_r$ : measured and the position reference respectively  
 $\omega$ : rotor angular speed  
 $\tau$ : torque command  
 $\tau_d$ : load torque  
 The sliding surface  $\sigma$  is defined as:

$$\sigma = \dot{e} + C \cdot e = (\dot{\theta}_r - \dot{\theta}) + C(\theta_r - \theta) \quad (7)$$

$C$ : a positive constant

From the second theorem of Lyapunov, the stability condition can be written as:

$$\frac{1}{2} \cdot \frac{d\sigma^2}{dt} = \sigma \cdot \dot{\sigma} \leq -K |\sigma| \quad (8)$$

Where:  $\frac{1}{2} \cdot \sigma^2 > 0$  (positive definite) is a Lyapunov function and  $K$  a positive constant. The control torque command is calculated by substituting  $\sigma$  and  $\dot{\sigma}$  in eq. (8) as following:

$$\tau = J \cdot \left[ \ddot{\theta}_r + C \cdot \dot{\theta}_r + \left( \frac{B}{J} - C \right) \cdot \omega + \frac{1}{J} \cdot \tau_d + K \cdot \text{sign}(\sigma) \right] \quad (9)$$

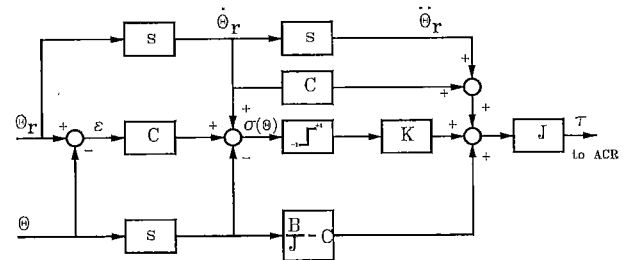


Fig. 6. Block diagram of the conventional SM controller.

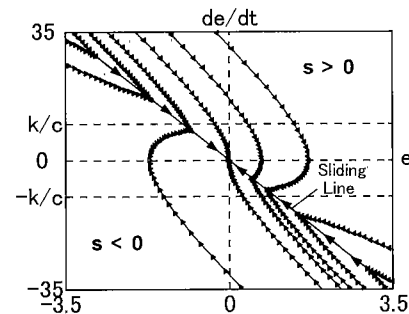


Fig. 7. Phase plane diagram in sliding mode.

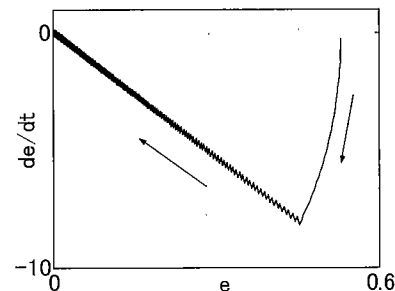


Fig. 8. Sliding line for conventional SM (simulation).

A block diagram of this conventional SM controller is shown in Fig. 6 and the phase plane representation in Fig. 7.

The problem with this conventional controller is that it has large chattering in the control output and the drive is very noisy. Furthermore, because of chattering, it is difficult to achieve small enough positioning error in steady state (see Fig. 8).

To reduce chattering the sign function (infinite gain) of the conventional SM is substituted with a finite gain  $K$  within a small boundary. This affects controller's robustness too, but still the controller will remain robust enough if gain  $K$  is chosen large enough.

An infinite or very large gain  $K$  increases chattering because the bandwidth of the ACR is not infinite. We assumed an ideal ACR and did not include it in the plant model, but this assumption holds as long as the bandwidth of the outer control loops do not exceed that of ACR. For this reason hardware implementation of ACR is recommended, such that the largest bandwidth possible can be achieved.

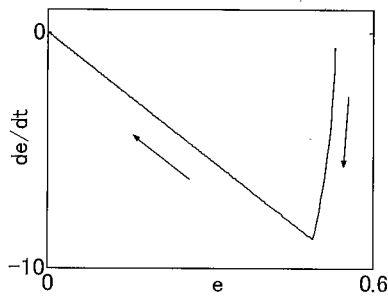


Fig.9. Sliding line for a finite gain controller (simulation).

The selection of a finite  $K$  gain affects the sliding surface as seen in the step response of the system shown in the phase plane in Fig. 8 and Fig. 9. In Fig. 8, which corresponds to the controller configuration shown in Fig. 6, it is obvious chattering after reaching sliding mode. By choosing a finite, appropriate value for  $K$  the chattering is greatly reduced (see Fig. 9).

The constant  $C$  basically determines the speed of response. It is the only parameter, which determines the dynamic of the system in SM. The choice of the constant  $C$  is also bounded from the ACR bandwidth and the encoder noise. Larger values of constant  $C$  tend to faster response, but if the bandwidth of the ACR is exceeded this will lead in chattering and it will deteriorate the controller performance.

To reduce greatly the steady state error an integral block is added, which forces the system in steady state toward a zero error positioning. This integral block tends to slow down the transient response of the control system. For this reason it is switched on only when the system approaches the final position. On one hand the sliding mode tracks the reference very fast ensuring a very small tracking error till the final positioning is reached and on the other hand the integral block, taking advantage of the small initial error, reduces it to zero very fast.

The gain  $K$  is switched to a larger value  $K1$  right before the position command reaches the desired final value. The condition of switching is detected when speed and acceleration signals of the position command have opposite signs and the speed of the motor reaches some hundred  $\text{min}^{-1}$ . This gain is returned to its previous value immediately after the final position is reached. This ensures a fast and precise stop of the servo. If a large gain will be applied all the time, chattering in the torque command will be inevitable.

At this point we have designed a controller, which has a very good tracking and reaches very fast the final position. The controller is also very robust to the outside disturbance or parameter uncertainties. Still the tracking performance can be improved if we consider the outside disturbance in the system. Mainly the outside disturbance is caused by friction changes and modeling it is not an easy task. Further, conditions in which a mechanism works are continuously changed. Therefore we see it appropriate to include a fuzzy type parameter adaptation algorithm to compensate for friction changes.

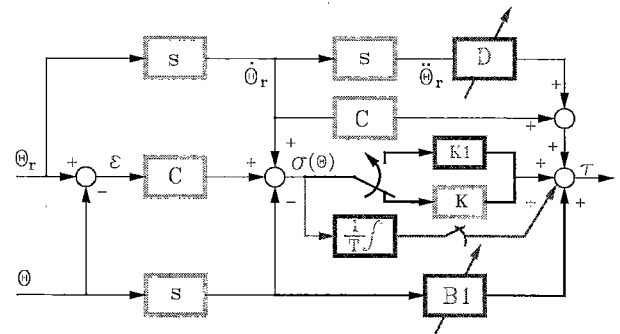


Fig.10. Block diagram of the new sliding mode integral controller with switched gains.

Based on  $\sigma$  and  $\dot{\sigma}$  as inputs, a fuzzy controller adjusts the gain  $B1$ , which includes the damping constant  $B$  in it. Initially the parameter is set in accordance with the result from the identification process described in Sec.3. Then the algorithm based on fuzzy control adapts parameter  $B$  to the real friction changes of the mechanism. This adaptation is important especially in case of the mechanisms that have a large  $B/J$  ratio (e.g. the ball-screw table used in our experiment). The algorithm uses the following fuzzy rules:

- (1) If  $\text{abs}(\sigma) < (\text{min pulses number})$  then (no gain change).
- (2) If  $\sigma < -(\text{min pulses number})$  then (increase gain fast).
- (3) If  $\sigma > (\text{min pulses number})$  then (decrease gain fast).
- (4) If  $\text{abs}(\sigma) < (\text{min pulses number})$  &  $d\sigma/dt > 0$  then (decrease gain slow).
- (5) If  $\text{abs}(\sigma) < (\text{min pulses number})$  &  $d\sigma/dt < 0$  then (increase gain slow).

For the implication, aggregation and defuzzification, the minimum, maximum and the largest of the maximum methods respectively are used.

A block diagram of the new sliding mode integral controller is shown in Fig.10. As seen in Fig.10 an additional gain  $D$  is added which multiplies the second derivative calculation of the position command. This is done in order to deal better with friction changes of the mechanism machine. This gain is proportionally adapted to the error magnitude in every sample time during the operation. In case of the ball-screw table friction characteristic during acceleration is different from that during deceleration and further more both are qualitatively different from the flywheel case.

Table 2. Servomotor.

Rated power [P]	200 W
Rated torque [T]	0.637 Nm (max. 1.91 Nm)
Rated speed [n]	3000 $\text{min}^{-1}$ (max. 5000 $\text{min}^{-1}$ )
Moment of inertia [J]	$2.16 \times 10^{-5} \text{ kg m}^2$
Rated current [I]	1.5 A (max. 4.5 A)
Encoder	16 bit serial encoder.

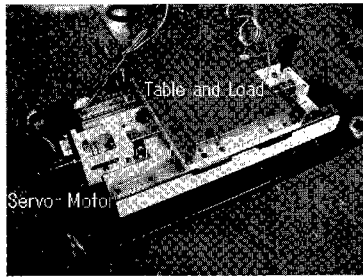


Fig. 11. Experimental ball screw table mechanism.

#### 4. Implementation and Experimental Results

Two main servo applications were targeted in this study, the flywheel and the ball-screw table (see Fig. 11).

The following data correspond to the experimental equipments used:

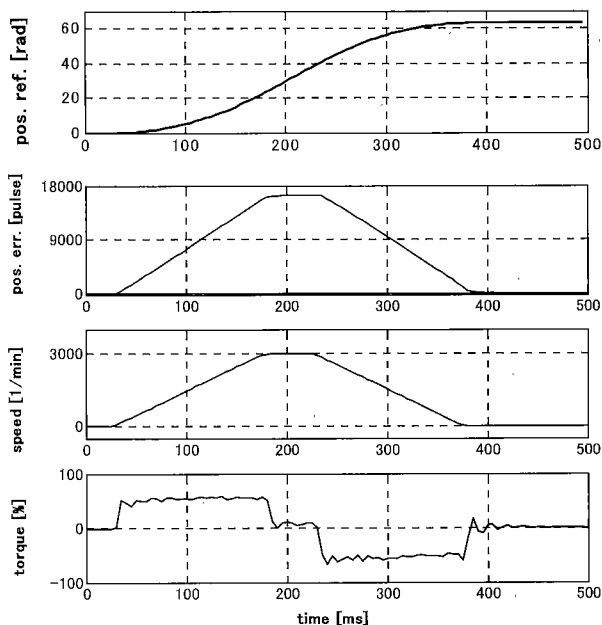


Fig. 12. Performance of the PI controller (Fly-wheel case).

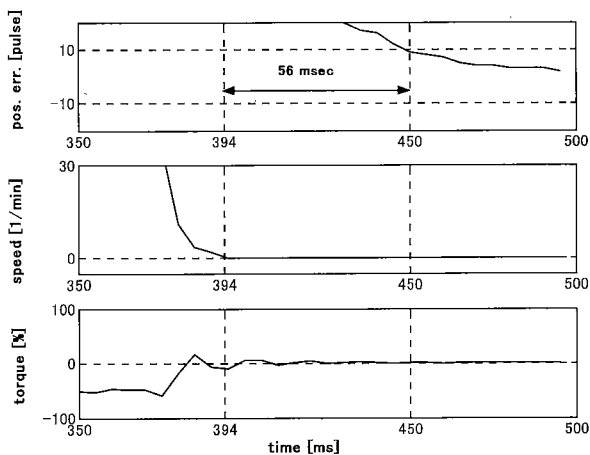


Fig. 13. Zoom of Fig. 12 waveforms near final position.

In Fig. 12 and Fig. 13 are shown the responses of the PI controller (cascade configuration with PI as speed controller and P as positioning controller). The torque and error data are recorded in the controller. It is seen that the tracking error is very large and the final position (less than 10 encoder pulses error) is reached in 56 ms.

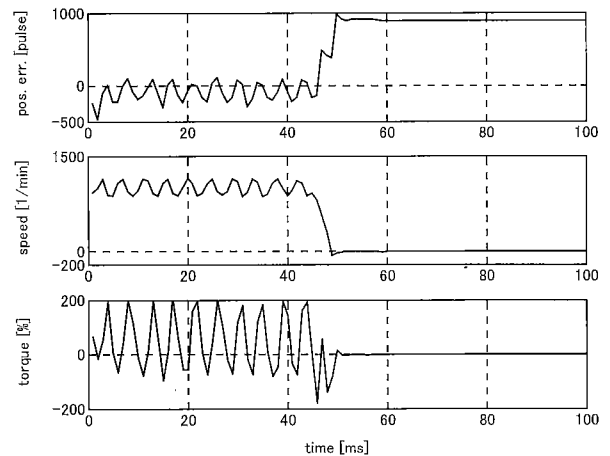


Fig. 14. Performance of conventional SMC (Fly-wheel case).

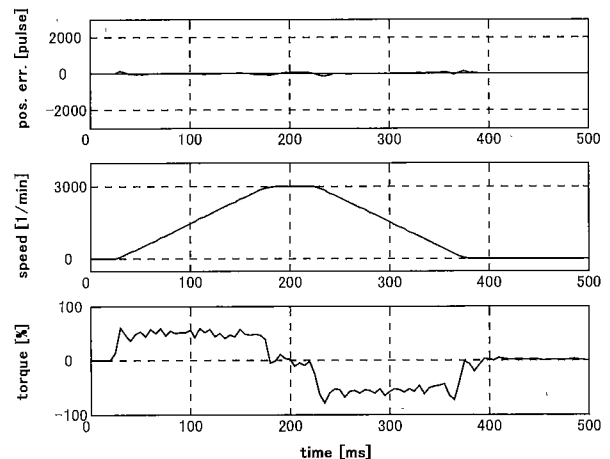


Fig. 15. Performance of the SMI controller (Fly-wheel case).

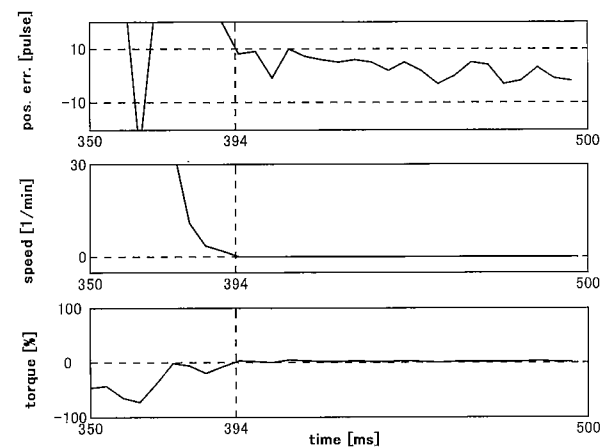


Fig. 16. Zoom of Fig. 15 waveforms near final position.

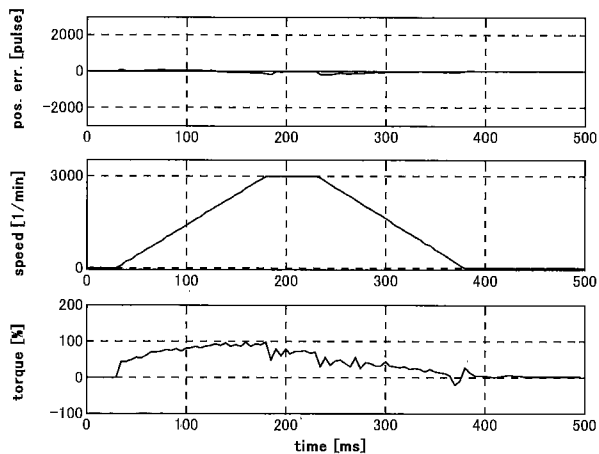


Fig. 17. Performance of the SMI controller (Ball-screw).

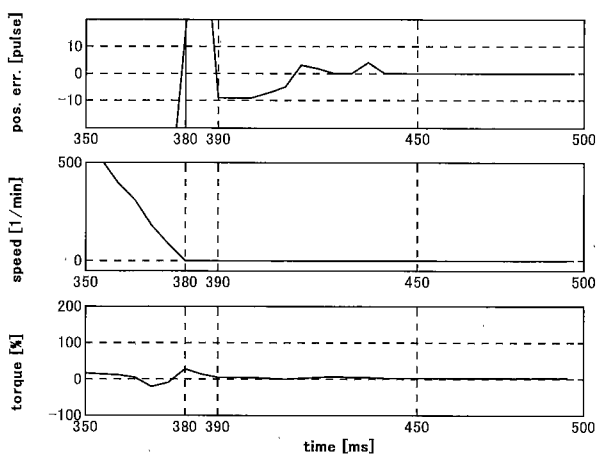


Fig. 18. Zoom of Fig. 17 waveforms near final position.

In Fig. 14 is shown the performance of the conventional sliding mode controller. The tracking error is much smaller than the PI controller but large torque ripples occur in the command output and the drive become noisy. Furthermore the steady state error requirement (10 encoder pulses) is not reached. As seen from Fig. 15 to Fig. 18 the new proposed controller has a very good tracking and fast positioning. The tracking error is about 100 times smaller than the PI controller and the positioning time at least 5-6 times shorter.

In Fig. 16 the error is smaller than 10 pulses immediately after the command speed reaches zero. On the other side the torque ripples are kept small.

## 5. Conclusions

In this paper a new controller based on the SM principles is proposed. Compared to the classical SM it shows improvements in chattering, zero steady state error and a small tracking error. Compared to a PI controller the experimental tests have shown that it is much faster during tracking and reaches the final position faster, which are two main requirements for a servo drive. Parameter adaptation, gain scheduling and integral action are used to cope with model uncertainties. To minimize chattering in the control output a boundary solution approach is implemented.

This study shows that the best control method for a servo drive is the one which combines different control approaches in one controller opposed to a single pure control approach.

(Manuscript received May 16, 2002,  
revised Nov. 27, 2002)

## References

- (1) V. Utkin: "Sliding mode control design principles and applications to electric drives", *IEEE T. IE*, Vol.40, No.4, pp.23-36 February (1993)
- (2) K. Sato, A. Shimokohbe, et al: "Positioning Performance of a Lead screw System with Six Kinds of Control Methods.- Basic Positioning Performance and Effect of Coulomb Friction on the Performance-", *Proc. Japan-China Symposium on advanced manufacturing Engineering*, pp.39-44 (1998)
- (3) T. Chern and Y. Wu: "Design of Brushless DC Position Servo Systems using Integral Variable Structure Approach", *IEEE Proc.-B*, Vol.140, No.1, pp.27-34 Jan. (1993)
- (4) P. Pillay, R. Krishnan: "Modeling, Simulation and Analysis of Permanent-Magnet Motor Drives", *IEEE T. IA*, Vol.25, No.2, pp.265-273 Mar.-Apr (1989)
- (5) R. DeCarlo, et al.: "Variable Structure Control of Nonlinear Multivariable Systems: A Tutorial", *IEEE Proc.*, Vol.76, No.3, pp.212-232 (1988)
- (6) H. Hashimoto, F. Harashima, et al.: "Brushless Servo Motor Control Using Variable Structure Approach", *IEEE T. IA*, Vol.24, No.1, pp.160-170 Jan.-Feb. (1988)
- (7) H. Choi, et al.: "Global Sliding Mode Control.-Improved Design for Brushless DC Motor-", *IEEE Control Systems Magazine*, pp.27-35 June (2001)

**Orges Gjini** (Member) was born in Tirana, Albania in 1970.



He received B.E degree from Polytechnic University of Tirana (PUT) in 1993 and M.E degree from the University of Tokyo in 2000, both in Electrical Engineering. He has been a member of the Faculty at PUT from 1993 until 1997. Since 2000 he joined Fuji Electric Co. R&D, Ltd. His research areas of interest are motor drives and control. He is a member of the Institute of Electrical Engineers of Japan.

**Takayuki Kaneko** (Member) was born in Yamagata, Japan



in 1974. He received B.E degree from National Institution for Academic Degrees in 1997 and M.E degree from the Nagaoka University of Technology in 1999. Since 1999, he joined Fuji Electric Co. Research and Development, Ltd. His research interests are motion control and power electronics. He is a member of the Institute of Electrical Engineers of Japan.

**Hiroshi Ohsawa** (Member) received his B.E degree in



March 1972 from the Department of Electrical Engineering, Chuo University. He joined Fuji Electric Co., Ltd. in April of the same year. He is engaged mainly in the development of variable speed drive systems for electric motors. At present he is with Power Electronics Development Division at Fuji Electric Co. R&D, Ltd. He is a member of the Institute of Electrical Engineers of Japan.